ATTITUDE SENSOR AND GYRO CALIBRATION FOR MESSENGER

Dan O'Shaughnessy
Applied Physics Laboratory*

Dr. Mark E. Pittelkau
Aerospace Control Systems, LLC†

Abstract

The Redundant Inertial Measurement Unit Attitude Determination/Calibration (RADICAL^{TM}) filter was used to estimate star tracker and gyro calibration parameters using MESSENGER telemetry data from three calibration events. We present an overview of the MESSENGER attitude sensors and their configuration is given, the calibration maneuvers are described, the results are compared with previous calibrations, and variations and trends in the estimated calibration parameters are examined. The warm restart and covariance bump features of the RADICAL^{TM} filter were used to estimate calibration parameters from two disjoint telemetry streams. Results show that the calibration parameters converge faster with much less transient variation during convergence than when the filter is cold-started at the start of each telemetry stream.

1 Introduction

The MErcury Surface, Space ENvironment, GEochemistry, and Ranging (MESSENGER) spacecraft was launched on 3 August 2004 to enter an orbit around Mercury in March 2011. The MESSENGER spacecraft carries two Galileo Avionica Autonomous Star Trackers (A-STR), designated ST1 and ST2, and a Northrop-Grumman Space Inertial Reference Unit (SIRU) for attitude determination. Each star tracker provides attitude measurements at a sample rate of 10 Hz, and has a specified end-of-life accuracy at 0.5 deg/sec of 4.5 arcsec 1σ cross-boresight and 41 arcsec 1σ around its boresight. The present cross-boresight accuracy of the star trackers appears to be about 3.2 arcsec (cross-boresight) and 29 arcsec (boresight) for 9 tracked stars. The SIRU comprises four hemispherical resonator gyroscopes (HRGs) and provides integrated rate measurements at a sample rate of 100 Hz.

Precise on-board attitude determination, reliable residual edit (outlier) testing, and long-term sensor performance trending require that the star trackers and SIRU be well calibrated. Calibration parameters include star tracker misalignments, and gyro biases, symmetric and asymmetric scale factors, and gyro axis misalignments. The initial misalignments of the star trackers and gyros are relatively large due to orbit insertion effects, such as launch shock, bulk thermal change, and outgassing. Long-term changes in parameters are due to the varying thermal environment, radia-

*Senior Staff, e-mail: daniel.oshaughnessy@jhuapl.edu, Tel: 240-228-3807
†Consultant. Associate Fellow AIAA, Senior Member IEEE. e-mail: mpittelkau@acsinnovations.com, URL: http://www.acsinnovations.com/, Tel: 540-751-1110, 35215 Greyfriar Drive, Round Hill, VA 20141-2395

tion, aging, and other factors. On MESSENGER, the thermal environment varies not only with attitude, but also with distance from the Sun over the course of the mission. The bias, scale factors, and misalignments therefore require periodic calibration to enable precise attitude determination. Calibration is also needed if the SIRU is power-cycled and if its redundant power supply is activated. Critical times when precise attitude is needed are during trajectory correction maneuvers, Mercury orbit insertion, and operations in orbit around Mercury. Calibration manevers are therefore planned at discrete intervals during the mission to ensure precision attitude determination during these critical events. The calibration maneuvers and requirements and constraints on the maneuvers are described in this paper. At Mercury, in particular, the calibration has to be performed quickly and efficiently with minimal telemetry due to the hazardous thermal environment at Mercury and the low telemetry bandwidth due to the long distance from Earth. Interruptions of science observations should also be minimized.

A Redundant Inertial Measurement Unit IMU (RIMU) is an IMU that has $n > 3$ active sense axes. Three-dimensional body angular rates are mapped to the sense axes of the gyros by a $3 \times n$ body-to-gyro mapping matrix. A three-dimensional measurement can be computed from the n gyro measurements by using the pseudo-inverse of the body-to-gyro mapping matrix. This matrix has a null space, which is to say that the n gyro measurements contain redundant information that is not observable in the computed three-dimensional measurement, and so the physical calibration parameters are not fully observable. The RIMU calibration filter [1, 2] features a null-space measurement update that provides full observability of the calibration parameters. This filter has been analyzed extensively [3, 5] and new calibration algorithms were developed in [4]. An Extended Kalman Filter (EKF) designed for calibration of a 3-axis IMU will calibrate only the linear combination of the parameters that is observable in attitude [1, 6, 7], which is sufficient for some applications [8, 9, 10, 11]. One problem with this approach is that the calibration parameters are not valid if one gyro fails or is deactivated. The RIMU calibration filter has the advantage that the physical parameters can be completely calibrated and to greater accuracy. Failure of a gyro does not invalidate the calibrated parameters. Furthermore, the null-space measurement, or parity vector, is used for failure detection [12].

The RIMU calibration filter originally used to calibrate MESSENGER [13, 14, 15] was implemented in Matlab. The calibration algorithm was re-implemented in C with several enhancements, and is called the Redundant IMU Attitude Determination and Calibration (RADICAL^{TM}) filter [16]. The RADICAL^{TM} software comprises core filter functions, a driver program, pre-processing functions, and Matlab support software for sensor simulation and for plotting and tabulating results. The core filter functions include Extended Kalman Filter functions, a command interface, intialization for cold and warm start, processing of disjoint telemetry streams, default and active parameter tables, advanced measurement error models, the null space measurement update, fault detection and performance monitoring functions, diagnostic output data, telemetry output in a choice of three different size but customizable packets, and several other features. The covariance matrix in a calibration filter can become ill conditioned during its initial convergence and in other situations. Therefore UD-factorized covariance algorithms are used in RADICAL^{TM} to ensure numerical stability and accuracy. The covariance matrix is never computed, except that certain elements of the covariance matrix are computed only for output and for convergence threshold tests. RADICAL^{TM} is suitable for real-time on-board calibration, automated ground processing of telemetry, and desktop analysis and design.

One feature of the RADICAL^{TM} calibration filter is that it can process disjoint or interrupted telemetry streams. The attitude estimate, attitude covariance, and attitude cross-covariance are reset when there is a break in the gyro data. The parameter covariance remains intact (in UD factorized form). This is called a "warm-start" of the calibration filter. In addition, a covariance "bump" can be applied to model uncertainty due to a change in the parameters since the epoch of

the previously processed telemetry stream. (A covariance bump can also be applied at any time during processing in RADICAL^{TM}.) A bump can also be applied to the attitude covariance. The covariance bump is simply a specified increase in the covariance of any estimated parameter or attitude, and is applied upon a warm start or at any time upon command. The bump is applied directly to the UD factors of the covariance matrix to ensure numerical accuracy and stability and for computational efficiency. The importance of being able to process disjoint telemetry streams and applying the covariance bump is that the filter does not have to be reinitialized, and the filter is nearly converged when the prior converged estimates and their covariance are used to warm start the filter. This can be of benefit in autonomous on-board calibration on future NASA missions. Convergence problems are avoided when a prior estimate and a small prior covariance are used to warm-start the filter. In addition, a shorter calibration maneuver may be sufficient to maintain convergence of the calibration parameters and their covariance. This can be of benefit during mission operations to reduce risk (for example, in the hot solar environment at Mercury), to reduce interruption of science operations, and to reduce the volume of telemetry dedicated to calibration. A calibration maneuver can also be segmented to avoid constraints.

Simulation results in [13] and the initial calibration from telemetry data reported in [14] demonstrate the efficacy of the RIMU calibration filter. The MESSENGER attitude sensors were calibrated on three other occasions, and the results from all four calibrations were reported in [15]. In this paper, we present calibration results using the RADICAL^{TM} software and telemetry from MESSENGER and compare the results with those reported in [15]. Results are presented to demonstrate the calibration filter's performance when processing disjoint telemetry streams. We also discuss the MESSENGER attitude sensor configuration and how the raw data is pre-processed to obtain RADICAL^{TM} readable files.

The results in this paper are intended to illustrate the efficacy of the RADICAL^{TM} calibration filter and to provide an unofficial but independent analysis of the attitude sensor and gyro calibration on MESSENGER.

2 Filter Parameters and Calibration Maneuver

2.1 Sensor Geometry

The locations of the star trackers and SIRU on the spacecraft are shown in Figure 1. The x, y, and z body-frame axes are also shown. The nominal mounting matrices for the star trackers and the IMU (the SIRU) are given by

$$\mathbf{T}_{\mathrm{b}}^{\mathrm{st1}} = \begin{bmatrix} 1 & 0 & 0 \\ 0 & -1 & 0 \\ 0 & 0 & -1 \end{bmatrix} \qquad \mathbf{T}_{\mathrm{b}}^{\mathrm{st2}} = \begin{bmatrix} 0 & 1 & 0 \\ 1 & 0 & 0 \\ 0 & 0 & -1 \end{bmatrix} \qquad \mathbf{T}_{\mathrm{b}}^{\mathrm{imu}} = \begin{bmatrix} -1 & 0 & 0 \\ 0 & 0 & 1 \\ 0 & 1 & 0 \end{bmatrix} \tag{1}$$

The two star trackers, ST1 and ST2, are mounted with parallel boresights in the $-z$-body axis direction, and ST2 is rotated 90 degrees relative to ST1. ST2 is a redundant star tracker and is normally off during the mission because the thermal control system cannot dissipate the heat of both star trackers. ST2 is on during calibration so that its relative alignment will be known to some level of accuracy in case it is ever needed during normal mission operations. The SIRU is mounted remotely from the star trackers, so thermal deformation is expected to appear in the estimated misalignments of the SIRU relative to the star trackers.

The RIMU error model derived in [5] is parameterized with three geometry matrices whose corresponding columns form an orthogonal triad fixed to each sense axis. The nominal geometry

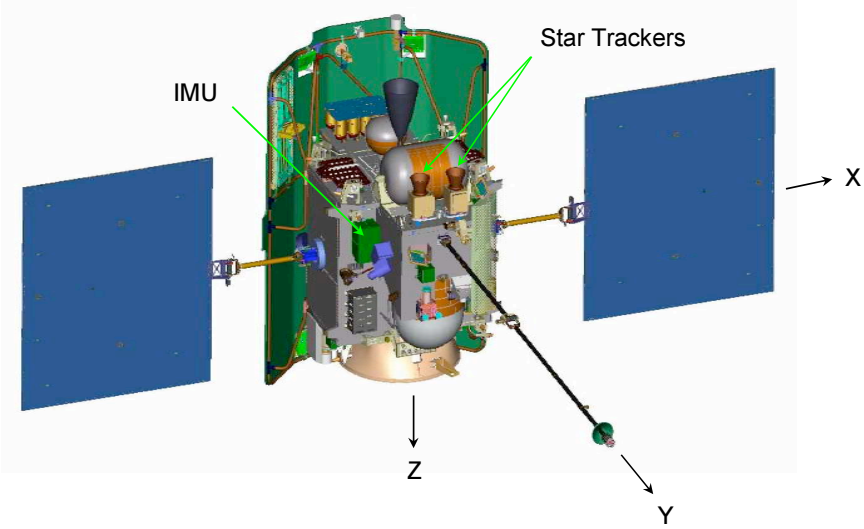

Figure 1. Drawing of MESSENGER showing sensor locations.

matrices for the octahedral arrangement of gyros in the SIRU are

$$\boldsymbol{U} = \frac{1}{\sqrt{6}}\begin{bmatrix} -2 & -2 & -2 & -2 \\ 1 & -1 & 1 & -1 \\ 1 & 1 & -1 & -1 \end{bmatrix} \qquad \boldsymbol{V} = \frac{1}{\sqrt{2}}\begin{bmatrix} 0 & 0 & 0 & 0 \\ -1 & -1 & -1 & -1 \\ 1 & -1 & -1 & 1 \end{bmatrix} \qquad \boldsymbol{W} = \frac{1}{\sqrt{3}}\begin{bmatrix} 1 & 1 & -1 & -1 \\ 1 & -1 & -1 & 1 \\ 1 & 1 & 1 & 1 \end{bmatrix} \tag{2}$$

where the columns of $\boldsymbol{W}$ are the sense axis direction vectors, and corresponding columns of $\boldsymbol{U}$, $\boldsymbol{V}$ and $\boldsymbol{W}$ form an orthogonal triad. The choice of $\boldsymbol{U}$ and $\boldsymbol{V}$ is arbitrary, but once chosen they should not be changed. The initial ground-based optical alignment parameters and the SIRU vendor's measured sense-axis direction vectors in $\boldsymbol{W}$ were used to produce the calibration results in [14, 15]. The measured $\boldsymbol{W}$ and the corresponding $\boldsymbol{U}$ and $\boldsymbol{V}$ matrices are slightly different from the nominal matrices.

2.2 Calibration Parameters

The physical gyro parameters that are estimated are the gyro biases $\boldsymbol{b}$, the symmetric scale factor vector $\boldsymbol{\lambda}$, an asymmetric scale factor vector $\boldsymbol{\mu}$, and sense-axis misalignment vectors $\boldsymbol{\delta_u}$ and $\boldsymbol{\delta_v}$. Each vector has $n = 4$ elements, one for each of the four sense axes of the SIRU. The misalignment $\boldsymbol{\delta}_{a_2}$ of ST2 is also estimated. ST1 is chosen to be the body reference sensor since it is normally the active star tracker, and so misalignments are not estimated for ST1. Thus the misalignment of ST2 is a relative misalignment.

The body-to-gyro mapping matrix is given by $\boldsymbol{G} = \boldsymbol{W}^T$. The corrected body-to-gyro mapping matrix is computed using the gyro error model [5]

$$\acute{\boldsymbol{W}} = \big(\boldsymbol{W} - \boldsymbol{V}\boldsymbol{\Delta_u} - \boldsymbol{U}\boldsymbol{\Delta_v}\big)\big(\boldsymbol{I} - \boldsymbol{\Lambda} - \mathbf{M}\big) \tag{3}$$

where $\boldsymbol{\Delta_u} = \mathrm{diag}(\boldsymbol{\delta_u})$, $\boldsymbol{\Delta_v} = \mathrm{diag}(\boldsymbol{\delta_v})$, $\boldsymbol{\Lambda} = \mathrm{diag}(\boldsymbol{\lambda})$, and $\mathbf{M} = \mathrm{diag}(\boldsymbol{\mu})$. Although the scale factor asymmetry $\boldsymbol{\mu}$ is estimated, there is no provision in MESSENGER's on-board software to use it.

2.3 Calibration Filter Initialization

The initial parameter estimates are zero, and the initial parameter estimation errors are assumed to be uniformly distributed on $[-L, L]$ as shown in Table 1. The variance of the initial parameter estimation error is set to $3L^2$, which reflects 3σ uncertainty. The attitude is initialized with the first valid star tracker measurement, and the attitude covariance is initialized according to the measurement error.

Although the star trackers transmit variances of their cross-boresight and boresight errors, the values are quantized too much to be useful [15]. Thus the present accuracy values stated in the Introduction are input to the calibration filter. These values are weighted in RADICAL^{TM} according to the number of tracked stars.

The process noises are 0.001 ppm/sec$^{1/2}$ (ppm = parts per million) for the scale factors, 0.001 arcsec/sec$^{1/2}$ for the gyro sense axis misalignments, and 0.002 arcsec/sec$^{1/2}$ for the ST2 misalignments. These allow the filter to track parameter variations and prevent the covariance from becoming ill conditioned or singular.

Table 1. Initial Parameter Distributions on $[-L, L]$

Parameter	**Symbol**	L	**Units**
bias	$\boldsymbol{b}$	3	deg/hr
symmetric scale factor	$\boldsymbol{\lambda}$	5000	ppm
asymmetric scale factor	$\boldsymbol{\mu}$	100	ppm
gyro sense axis misalignment	$\boldsymbol{\delta_u}$	3600	arcsec
gyro sense axis misalignment	$\boldsymbol{\delta_v}$	3600	arcsec
ST2 misalignment	$\boldsymbol{\delta}_{a2}$	1800	arcsec

2.4 IMU Data Pre-Processing

The internal SIRU clock is not synchronized with the bus clock, so the actual sampling time drifts relative to the bus clock [15]. Both the actual sampling time and the time tag counter drift relative to the bus clock. (Time tag counter reset commands only set the time tag counter to zero, and the time of the reset is uncertain. Time tag counter resets have not been issued to the IMU in the MESSENGER telemetry since a software load on 11 October 2005.) As the IMU clock drifts relative to the bus clock, the time tag error increases almost linearly from 0 to 10 msec and then immediately back to 0. As the SIRU clock and the bus clock edges pass each other, the time tag error is close to zero. Clock noise then causes a spate of missing and repeated samples. The IMU data is sampled at 100 Hz and processed prior to filtering to remove repeated samples and to correct the SIRU time tags as described in [15]. In the calibration filter, the SIRU telemetry is shifted 0.11 sec relative to the star tracker data for time alignment, and an additional 5 msec correction is performed within the calibration filter. This time alignment was found to minimize the measurement residuals in the calibration filter.

2.5 Calibration Maneuvers

The calibration maneuvers in Figure 2 are similar to the originally proposed maneuvers in [13]. The maneuver shown in Figure 2a is +90 degrees rotation about the body x-axis, ±30 deg rotation about the y-axis, ±30 deg rotation about the z-axis, and −90 deg rotation about the x-axis.

The maximum angular rate is ±0.3 deg/sec. A proposed alternate calibration maneuver shown in Figure 2b is a rotation of ±30 deg about each axis in sequence at a maximum angular rate of ±0.3 deg/sec. The duration of each sequence is 4000 sec. These calibration maneuvers are designed so that the calibration parameters are distinguishable. (It is less precise to say that the maneuver makes the parameters observable.) The maneuvers are designed also so that the star trackers avoid the Sun and that sufficient power is available from the solar arrays, and so that the acceleration and momentum of the spacecraft are within the capabilities of the reaction wheels. The ramped angular rate helps to average out scale factor nonlinearity in the gyros. These maneuvers are designed for use outside of 0.85 astronomical units (AU) from the Sun so that thermal constraints on the spacecraft are not violated. A complete history of calibration maneuvers executed on MESSENGER can be found in [15].

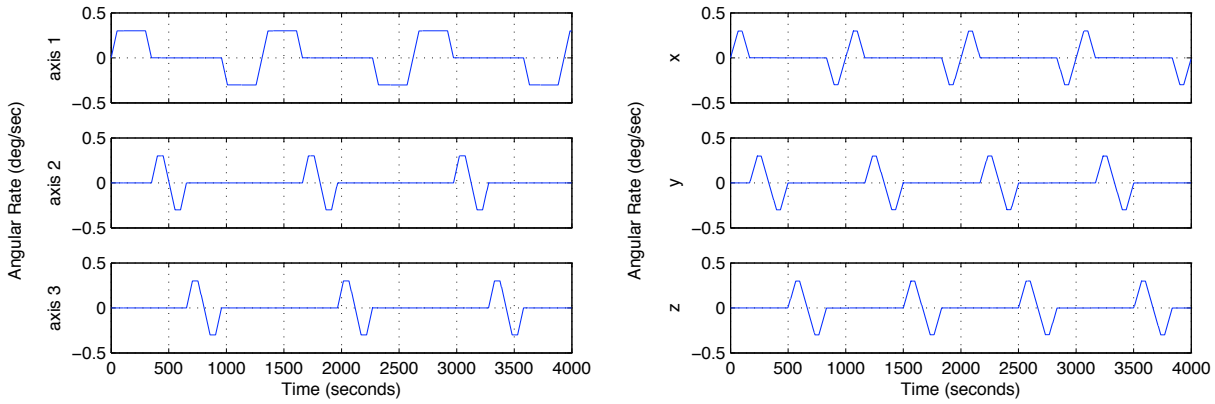

(a) Originally proposed maneuver

(b) Alternate maneuver

Figure 2. Two originally proposed calibration maneuvers.

Inside of 0.85 AU the y-axis of the spacecraft must be within 12 degrees of the direction to the Sun. The actual calibration maneuver from 2006216 (year 2006 and day-of-year 216), where the spacecraft is within 0.85 AU, is shown in Figure 3. Calibration maneuvers on 2005300 and 2005301 are nearly the same and so are not shown. These maneuver sequences are ±10 deg about the x-axis, ±10 deg about the z-axis, and ±360 deg about the y-axis. The current ±360 deg rotation angle about the z-axis makes the calibration maneuver excessively long; ±60 degrees would be sufficient. It will be seen in the results that the calibration parameters have mostly converged in 60 min, which is just after the y-axis angular rate changes sign as shown in Figure 3.

3 Results

The calibration parameters were estimated using telemetry from calibration maneuvers on 2005300, 2005301, and 2006216. The final estimates at the end of the calibration maneuvers are shown in Tables 2 through 7. Standard deviations computed from the filter's UD factorized covariance matrix are also shown in the tables. Results from the calibration maneuver on 2006216 are shown in Figures 4 through 6. These figures show the star tracker residuals, null space measurement residuals, and estimated parameters and standard deviations of error (±1σ bounds) at each measurement update over the course of the maneuver. The standard deviations are computed from the calibration filter's UD-factors of the covariance matrix. Graphs of results for telemetry on 2005300 and 2005301 are similar to those for 2006216 and are not shown. These results are consistent with those in [14, 15], except that the estimated $\boldsymbol{\delta_u}$ and $\boldsymbol{\delta_v}$ in [15] appear to be inconsistent for

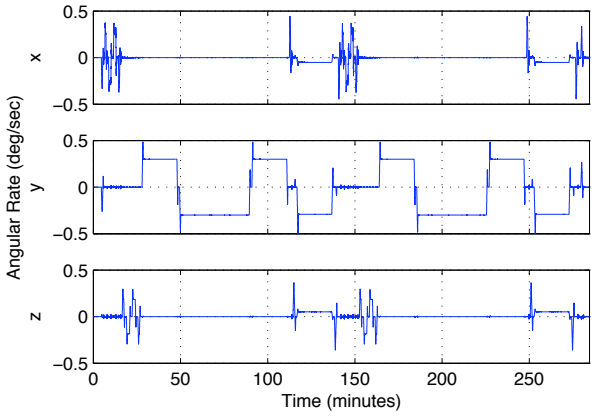

Figure 3. Calibration maneuver on 2005300, 2005301, and 2006216.

some yet unknown reason. A close examination of the star tracker residuals in Figures 4c,d show that the residual errors increases with non-zero y-axis angular rate of the spacecraft. These errors are above the specification for the star tracker. The cause of the excess error is unclear at this time.

3.1 Processing Disjoint Telemetry Streams

The RADICAL^{TM} calibration filter is capable of processing disjoint telemetry streams, which has several advantages as explained in the Introduction. This capability is demonstrated here using telemetry from 2005301 and 2006216. The telemetry from 2005301 was processed first and then the warm restart was performed with a covariance bump applied when the filter started to process telemetry from 2006216. Typical changes in the parameters lead us to choose the following standard deviations to use in the covariance bump: ST2 misalignments: 50 arcsec (x-axis), 10 arcsec (y and z axes); gyro bias: 0.05 deg/hr; symmetric scale factor: 75 ppm (500 ppm for gyro B); asymmetric scale factor: 8 ppm (30 ppm for gyro D); gyro axis misalignments: 15 arcsec. The fourth row of Tables 2 through 7 show the estimates at the end of the maneuver on 2006216. These estimates are slightly different from those estimated using telemetry from only 2006216, and a few of the final standard deviations are slightly smaller. Graphs of the estimates and their covariance confirm that the variations in the parameters are small as the parameters and their covariance reconverge after the warm start with the covariance bump applied. Examples are in Figure 7 and Figure 8b. In Figure 7, the estimates converge more smoothly than those in Figure 6a,c (which started from a large initial covariance) and the 1σ bounds are less than those in Figure 6b,d. In Figure 8b the star tracker misalignment exhibits only a small initial transient. The remaining variation is due to temperature, which will be discussed below.

3.2 Calibration Parameter Variations

Turning the SIRU off and on, or changing power supplies in the SIRU, causes significant changes in the gyro parameters. The change is less when turning the same power supply off and on. The A power supply (designated PPSMA) is the primary unit. The B power supply (PPSMB) was used only during calibration maneuvers on 2004380 and 2005300. As can be seen in the tabulated data, the estimated gyro parameters change significantly from 2005300 to 2005301 and exhibit less change from 2005301 to 2006216. The change in the parameters is also seen in the results reported in [15]. Although it is useful to obtain an early calibration using the B power supply, the SIRU should remain on the A power supply during and after the final calibration prior to entering Mercury orbit.

3.3 Temperature Effect on Misalignment

The thermal control system was designed to radiate heat from only one active star tracker. When two trackers are on, as they are during the calibration maneuvers, the temperature increases at the mounting of the star trackers and at the detectors when the thermo-electric coolers reach their maximum capacity. Figure 8 shows that the estimated ST2 misalignments vary almost linearly with time as the temperature increases. This change in the misalignments was noted previously [15]. The correlation of misalignment and baseplate temperature of the star trackers is evident in Figure 9. The process noise on the modeled ST2 misalignment allows the calibration filter to track the varying misalignment. Because the covariance of the misalignment estimate converges rapidly, the estimate at about 25 minutes after calibration (before significant thermal distortion occurs) is close to the actual misalignment when operating with only ST2, since the temperature will not change when only ST2 is in operation. ST1 will normally be off if ST2 becomes the primary star tracker.

4 Conclusion

The Redundant IMU Attitude Determination and Calibration (RADICAL$^{\text{TM}}$) filter is designed to fully calibrate redundant inertial measurement units, which comprise more than three active sense axes. The RADICAL$^{\text{TM}}$ calibration filter was used to process telemetry data from the MESSENGER spacecraft to estimate gyro calibration parameters and star tracker misalignments. The calibration results reported in this paper are consistent with previously reported results. Results from a more recent set of telemetry are also reported in this paper.

The RADICAL$^{\text{TM}}$ filter has the capability to process disjoint telemetry streams without having to reinitialize the filter at the start of each stream. Only the attitude and attitude covariance and cross-covariance are reinitialized. A small covariance "bump" (or increase) is applied at the start of each telemetry stream after the first to model changes in the parameters since the previous stream. Results show that this method is effective and allows faster and smoother convergence of the parameters and their covariance when processing disjoint telemetry streams, including those separated by long time spans.

Acknowledgement

The second author thanks Dr. Sean Solomon of the Carnegie Institution of Washington, and Dr. Tom Strikwerda, Dan O'Shaughnessy (the first author), and Dr. Wayne Dellinger of the Applied Physics Laboratory, for providing telemetry data and support to conduct the analysis reported in this paper. This pro bono work was undertaken for the mutual benefit of Aerospace Control Systems Engineering and Research http://www.acsinnovations.com/, the Applied Physics Laboratory, and the MESSENGER mission.

Table 2. Estimated ST2 misalignment $\boldsymbol{\delta}_{a2}$, arcsec

Date	**Year-Day**	x-**axis**		y-**axis**		z-**axis**	
		δ_1	σ_{δ_1}	δ_2	σ_{δ_2}	δ_3	σ_{δ_3}
Oct 27, 2005	2005300	1323.7	0.06	−637.1	0.06	−428.9	0.17
Oct 28, 2005	2005301	1325.1	0.06	−636.2	0.06	−427.0	0.17
Aug 04, 2006	2006216	1331.2	0.06	−635.5	0.06	−430.2	0.17
2005301–2006216		1331.2	0.06	−635.5	0.06	−430.3	0.17

Table 3. Estimated bias $\boldsymbol{b}$, deg/hr

Date	Year-Day	Gyro A		Gyro B		Gyro C		Gyro D	
		b_1	σ_{b_1}	b_2	σ_{b_2}	b_3	σ_{b_3}	b_4	σ_{b_4}
Oct 27, 2005	2005300	0.3530	0.0024	−0.0536	0.0025	0.0964	0.0025	−0.0400	0.0025
Oct 28, 2005	2005301	0.5312	0.0023	−0.0679	0.0024	0.0658	0.0025	−0.0465	0.0024
Aug 04, 2006	2006216	0.5026	0.0022	−0.0997	0.0023	0.0871	0.0024	−0.0711	0.0023
2005301–2006216		0.5013	0.0022	−0.1008	0.0023	0.0820	0.0023	−0.0758	0.0023

Table 4. Estimated symmetric scale factor $\boldsymbol{\lambda}$, ppm

Date	Year-Day	Gyro A		Gyro B		Gyro C		Gyro D	
		λ_1	σ_{λ_1}	λ_2	σ_{λ_2}	λ_3	σ_{λ_3}	λ_4	σ_{λ_4}
Oct 27, 2005	2005300	77.9	3.5	314.7	4.2	348.6	3.4	701.8	4.2
Oct 28, 2005	2005301	295.5	3.4	29.1	4.0	558.5	3.3	362.7	4.1
Aug 04, 2006	2006216	326.4	3.4	−261.4	4.0	602.8	3.3	358.7	4.0
2005301–2006216		323.9	3.4	−265.9	4.0	590.4	3.3	343.7	4.0

Table 5. Estimated asymmetric scale factor $\boldsymbol{\mu}$, ppm

Date	Year-Day	Gyro A		Gyro B		Gyro C		Gyro D	
		μ_1	σ_{μ_1}	μ_2	σ_{μ_2}	μ_3	σ_{μ_3}	μ_4	σ_{μ_4}
Oct 27, 2005	2005300	6.2	3.4	−38.1	3.4	−55.8	3.0	4.0	3.3
Oct 28, 2005	2005301	−14.4	3.4	7.9	3.3	7.5	2.9	−39.5	3.2
Aug 04, 2006	2006216	−17.7	3.2	10.6	3.1	−1.5	2.9	−27.5	3.1
2005301–2006216		−13.5	3.0	14.1	2.9	6.3	2.7	−19.8	3.1

Table 6. Estimated gyro misalignments $\delta_{\boldsymbol{u}}$, arcsec

Date	Year-Day	Gyro A		Gyro B		Gyro C		Gyro D	
		$\delta_{\boldsymbol{u}_1}$	$\sigma_{\delta_{\boldsymbol{u}_1}}$	$\delta_{\boldsymbol{u}_2}$	$\sigma_{\delta_{\boldsymbol{u}_2}}$	$\delta_{\boldsymbol{u}_3}$	$\sigma_{\delta_{\boldsymbol{u}_3}}$	$\delta_{\boldsymbol{u}_4}$	$\sigma_{\delta_{\boldsymbol{u}_4}}$
Oct 27, 2005	2005300	513.2	0.7	461.4	0.7	833.4	0.7	840.9	0.7
Oct 28, 2005	2005301	492.9	0.7	477.0	0.7	851.7	0.7	815.9	0.7
Aug 04, 2006	2006216	489.9	0.7	482.6	0.7	862.6	0.7	816.9	0.7
2005301–2006216		490.1	0.7	482.6	0.7	861.8	0.7	816.9	0.7

Table 7. Estimated gyro misalignments $\delta_{\boldsymbol{v}}$, arcsec

Date	Year-Day	Gyro A		Gyro B		Gyro C		Gyro D	
		$\delta_{\boldsymbol{v}_1}$	$\sigma_{\delta_{\boldsymbol{v}_1}}$	$\delta_{\boldsymbol{v}_2}$	$\sigma_{\delta_{\boldsymbol{v}_2}}$	$\delta_{\boldsymbol{v}_3}$	$\sigma_{\delta_{\boldsymbol{v}_3}}$	$\delta_{\boldsymbol{v}_4}$	$\sigma_{\delta_{\boldsymbol{v}_4}}$
Oct 27, 2005	2005300	259.4	1.0	−221.5	0.8	−246.9	1.0	219.3	0.8
Oct 28, 2005	2005301	329.1	0.9	−298.7	0.8	−306.6	0.9	310.9	0.8
Aug 04, 2006	2006216	335.9	0.9	−304.6	0.8	−315.5	0.9	318.2	0.8
2005301–2006216		334.7	0.9	−306.2	0.8	−310.7	0.9	322.5	0.8

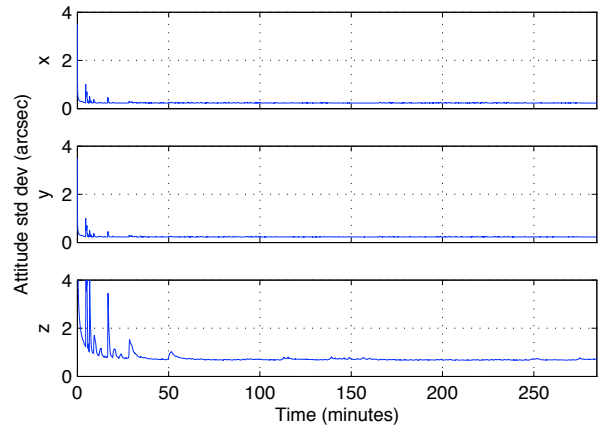

(a) Attitude error 1σ bounds

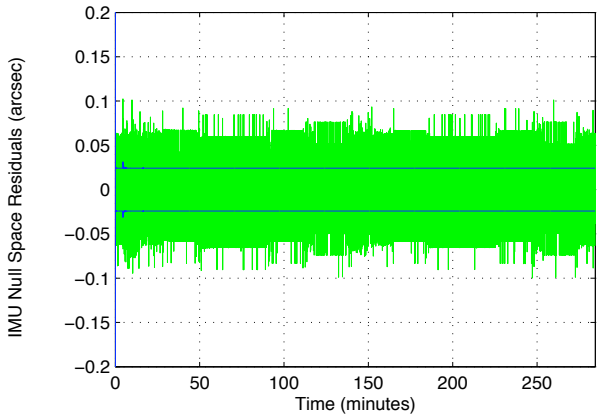

(b) Null-space residuals and $\pm 1\sigma$ bounds

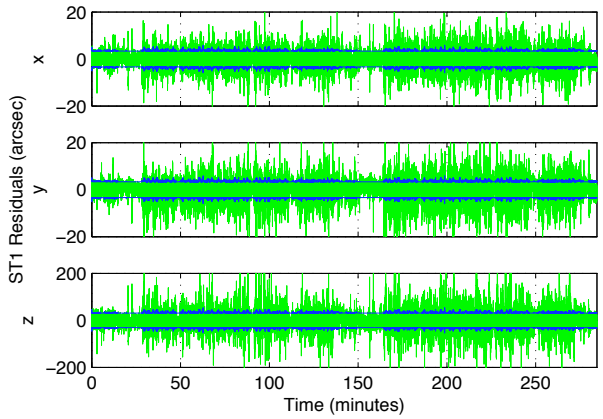

(c) Star Tracker 1 residuals and $\pm 1\sigma$ bounds

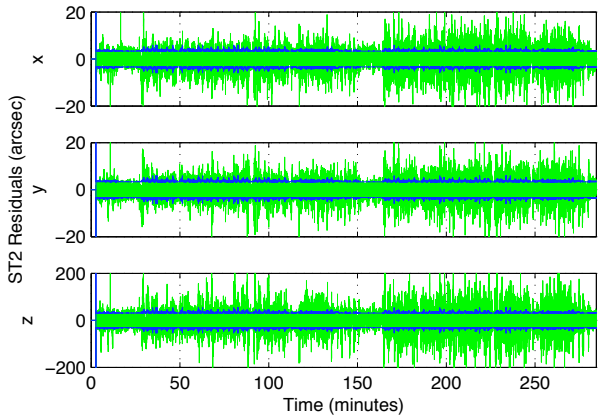

(d) Star Tracker 2 residuals and $\pm 1\sigma$ bounds

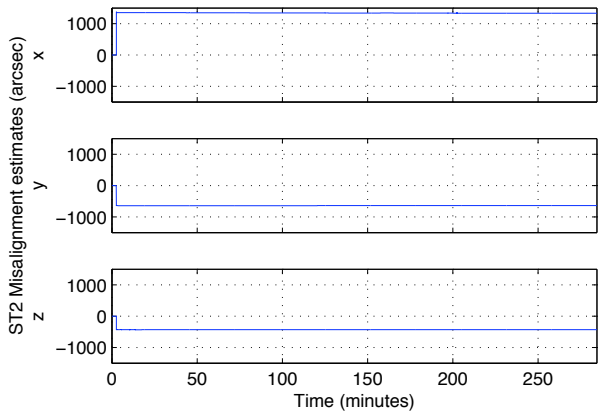

(e) Star tracker 2 alignment estimates

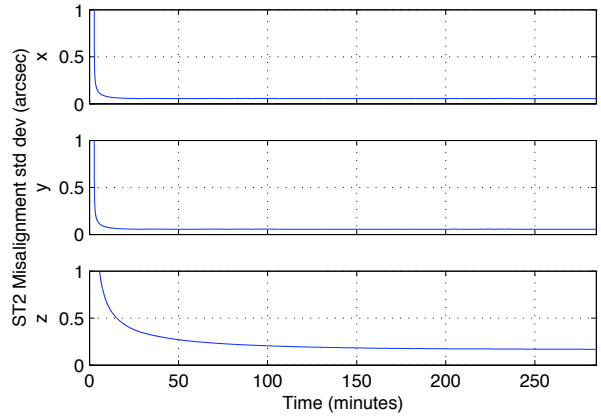

(f) Star tracker 2 alignment 1σ bounds

Figure 4. (a) Attitude 1σ bounds. (b) null space measurement residual and $\pm 1\sigma$ bounds. (c) ST1 residuals and $\pm 1\sigma$ bounds. (d) ST2 residuals and $\pm 1\sigma$ bounds. ST2 alignment (e) estimates and (f) standard deviations.

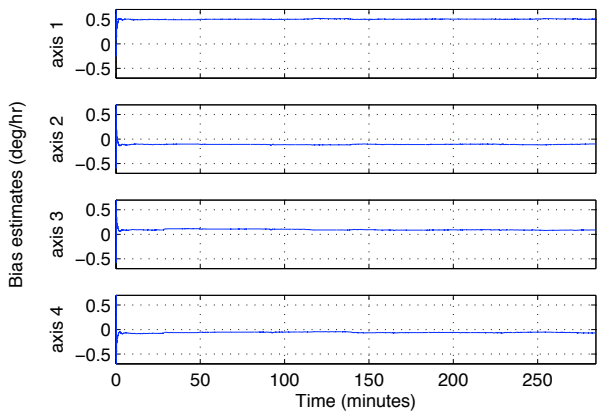

(a) Gyro bias b estimates

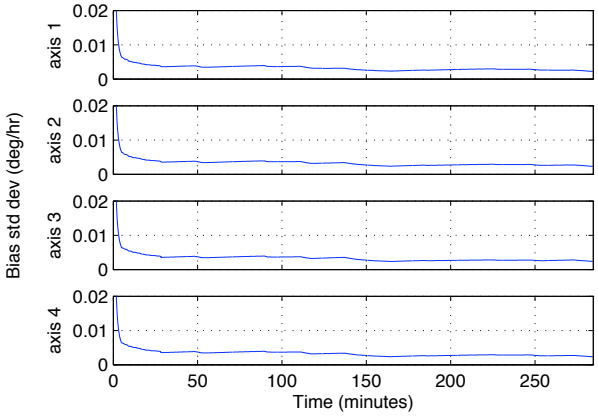

(b) Gyro bias 1σ bounds

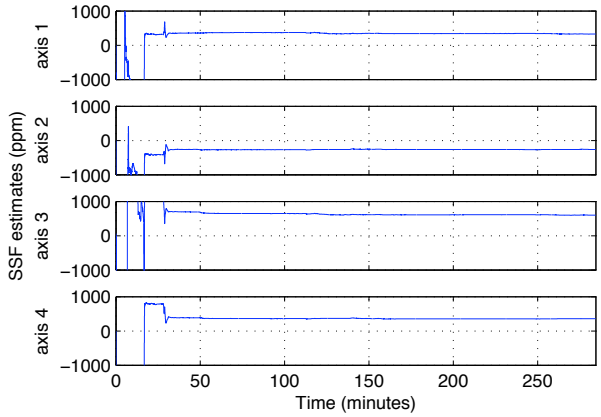

(c) ssf λ estimates

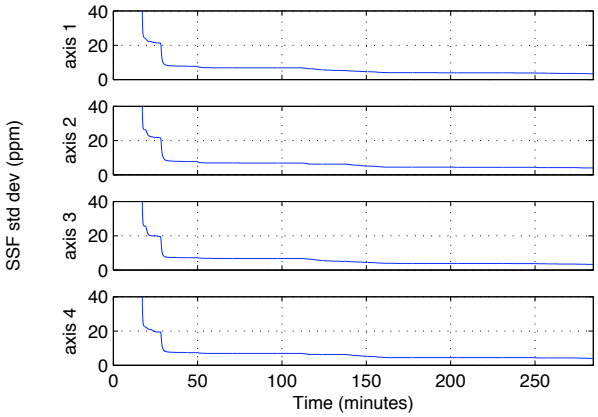

(d) ssf 1σ bounds

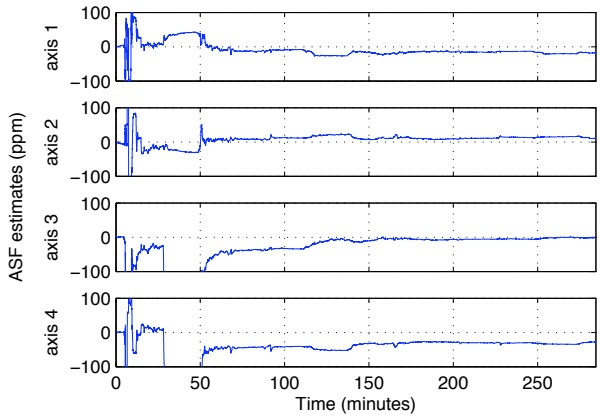

(e) asf μ estimates

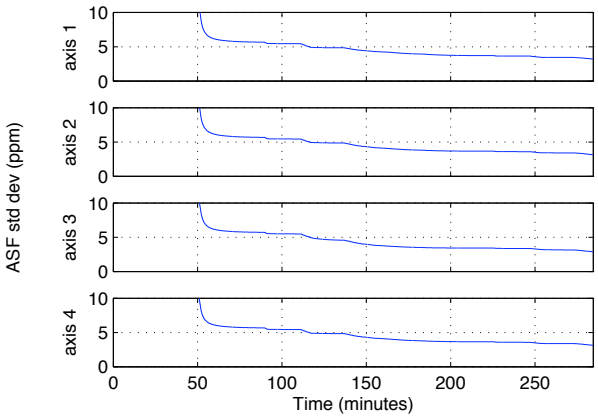

(f) asf 1σ bounds

Figure 5. Gyro bias (a) estimates and (b) standard deviations. Symmetric scale factor (c) estimates and (d) standard deviations. Asymmetric scale factor (e) estimates and (f) standard deviations.

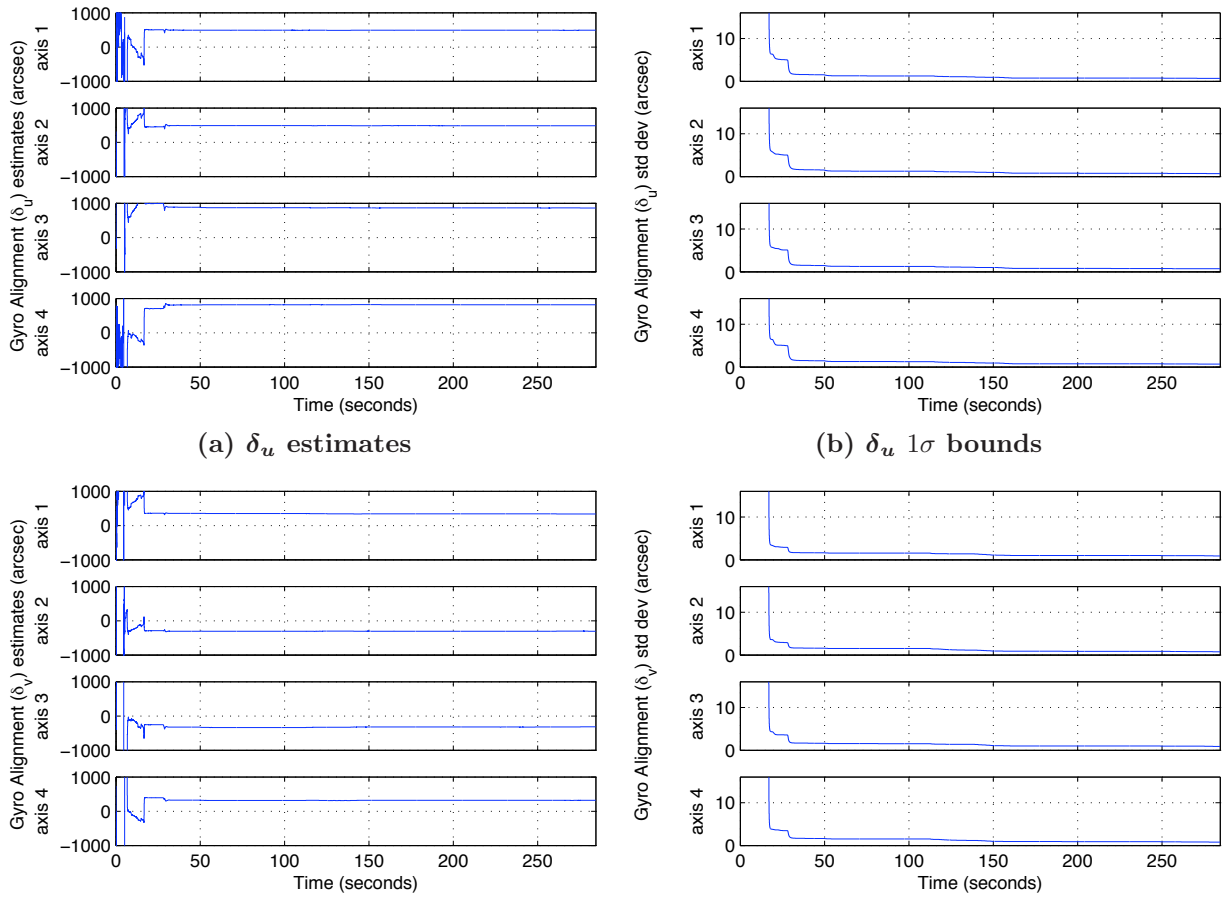

(a) $\boldsymbol{\delta_u}$ estimates **(b) $\boldsymbol{\delta_u}$ 1σ bounds**

(c) $\boldsymbol{\delta_v}$ estimates **(d) $\boldsymbol{\delta_v}$ 1σ bounds**

Figure 6. Gyro axis misalignment $\boldsymbol{\delta_u}$ (a) estimates and (b) standard deviations. Gyro axis misalignment $\boldsymbol{\delta_v}$ (c) estimates and (d) standard deviations.

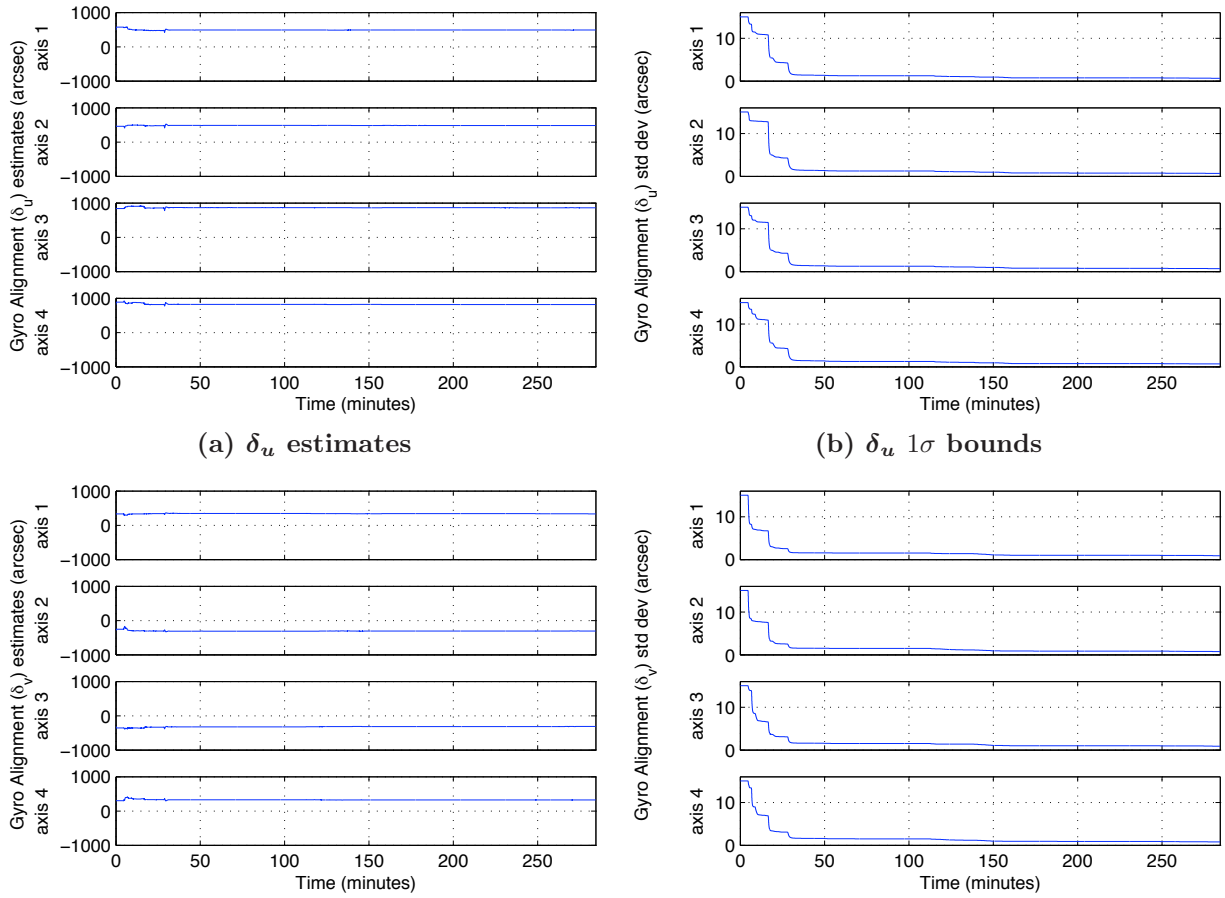

(a) $\boldsymbol{\delta_u}$ estimates **(b) $\boldsymbol{\delta_u}$ 1σ bounds**

(c) $\boldsymbol{\delta_v}$ estimates **(d) $\boldsymbol{\delta_v}$ 1σ bounds**

Figure 7. Gyro axis misalignment $\boldsymbol{\delta_u}$ (a) estimates and (b) standard deviations. Gyro axis misalignment $\boldsymbol{\delta_v}$ (c) estimates and (d) standard deviations. Estimates from telemetry on 2006216 are a continuation of those on 2005301 using the warm start and covariance bump features of the RADICAL$^{\text{TM}}$ calibration filter.

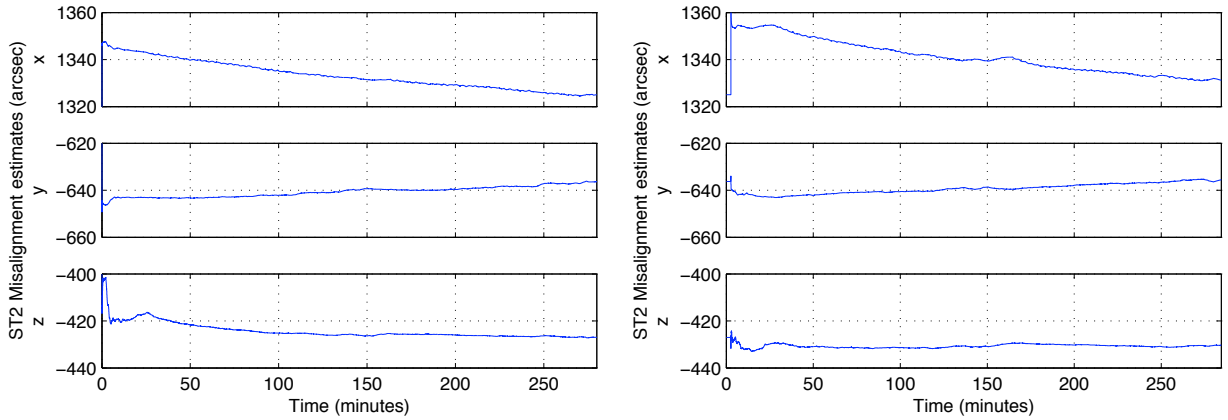

(a) Date: 2005301 **(b) Date: 2006216**

Figure 8. Temperature-varying ST2 misalignments. Estimates from telemetry on 2006216 are a continuation of those on 2005301 using the warm start and covariance bump features of the RADICAL^{TM} calibration filter.

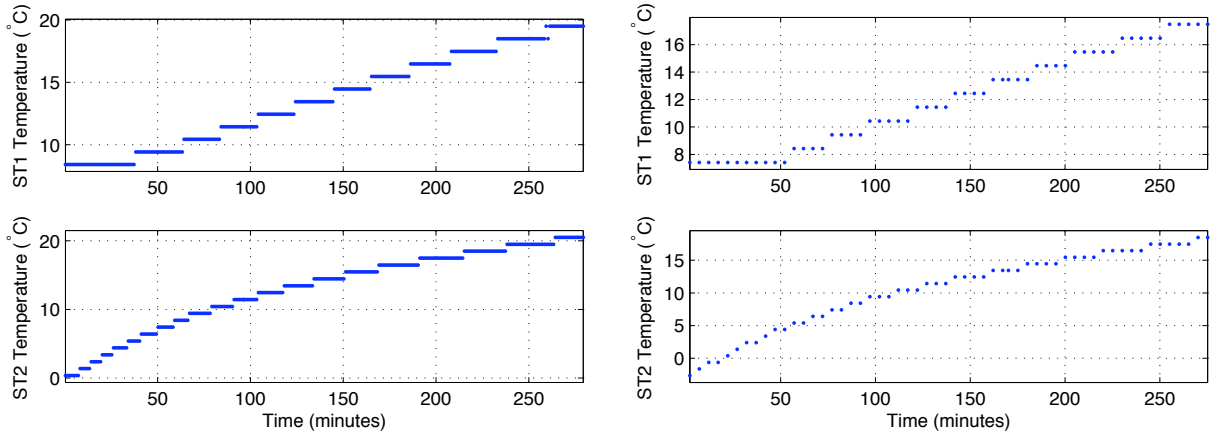

(a) ST1 temperature profile **(b) ST2 temperature profile**

Figure 9. Star tracker baseplate temperatures (a) ST1 and (b) ST2.

References

[1] Pittelkau, M. E., "Calibration and Attitude Determination with Redundant Inertial Measurement Units", *AIAA Journal of Guidance, Control, and Dynamics*, Vol. 28, No. 4, Jul–Aug 2005, pp. 743–752. 2

[2] Pittelkau, M. E., "Attitude Determination and Calibration with Redundant Inertial Measurement Units", AAS 04-116, AAS/AIAA Space Flight Mechanics Meeting, Maui, HI, 8–12 Feb 2004, in *Advances in the Astronautical Sciences*, Vol. 119, Part 1, 2004. 2

[3] Pittelkau, M. E., "RIMU Misalignment Vector Decomposition", AIAA-2004-4856, AAS/AIAA Astrodynamics Specialists Conference, Providence, RI, 16–19 Aug, 2004. 2

[4] Pittelkau, M. E.; "Cascaded and Decoupled RIMU Calibration Filters", *AAS Journal of the Astronautical Sciences*, Vol. 54, Nos. 3–4, Jul–Dec 2007. 2

[5] Pittelkau, M. E., "Observability and Calibration of a Redundant Inertial Measurement Unit (RIMU)", Paper No. AAS 05-105, *AAS/AIAA Space Flight Mechanics Meeting*, Copper Mountain, CO, 23–27 Jan 2005, in *Advances in the Astronautical Sciences*, Vol. 120, Part 1, 2005, pp. 71–84. 2, 3, 4

[6] Pittelkau, M. E.; "Recent Advances in Calibration of Redundant Inertial Measurement Units", *Flight Mechanics Symposium*, NASA/GSFC, NASA/CP-2005-212789, 18–20 Oct 2005. [online] 2

[7] Pittelkau, M. E.; "Advances in Attitude Determination With Redundant Inertial Measurement Units", Paper No. AAS 06-110, 2006 AAS/AIAA Spaceflight Mechanics Meeting, Tampa, FL, Jan 2006, *Advances in the Astronautical Sciences*, Vol. 124, Part 1, 2006, pp. 163–178. 2

[8] Gray, C. W.; Herman, L. K. ; Kolve, D. I.; Westerlund, G. L.; "On-Orbit Attitude Reference Alignment and Calibration", *Proceedings of the 13th Annual Rocky Mountain Guidance and Control Conference*, Keystone, CO, 3–7 Feb 1990, Paper AAS 90-042, in *Advances in the Astronautical Sciences*, Vol. 72, 1990, pp. 275–292. 2

[9] Bayard, D.; "An Overview of the Pointing Control System for NASA's Space Infra-Red Telescope Facility (SIRTF)", Paper No. AIAA-2003-5832, AIAA Guidance, Navigation, and Control Conference and Exhibit, Austin, TX, 11–14 Aug 2003. 2

[10] Wong, E. C.; Breckenridge, W. G.; "An Attitude Control Design for the Cassini Spacecraft", Paper No. AIAA-95-3274, Proceedings of the AIAA Guidance, Navigation, and Control Conference, Baltimore, MD, 7–10 Aug 1995, Part 2, pp. 931–945. 2

[11] Lee, A. Y.; Hanover, G.; "Cassini Spacecraft Attitude Control System Flight Performance", Paper No. AIAA 2005-6269, AIAA Guidance, Navigation, and Control Conference and Exhibit, San Francisco, CA, 15–18 Aug 2005. 2

[12] Daly, K. C.; Gai, E.; Harrison, J. V.; "Generalized Likelihood Test for FDI in Redundant Sensor Configurations", AIAA Journal of Guidance and Control, Vol. 2, No. 1, Jan–Feb 1979, pp. 9–17. 2

[13] Pittelkau, M. E., "MESSENGER Calibration", Technical Memorandum SRM-03-089, The Johns Hopkins University Applied Physics Laboratory, 24 Dec 2003. 2, 3, 5

[14] Pittelkau, M. E., "MESSENGER Attitude Sensor Calibration", Technical Memorandum SEG-04-060, The Johns Hopkins University Applied Physics Laboratory, 30 Sep 2004. 2, 3, 4, 6

[15] O'Shaughnessy, D. J.; Vaughan, R. M.; Haley, D. R.; H S. Shapiro, "MESSENGER IMU Interface Timing Issues and In-Flight Calibration Results", Paper No. AAS 06-086, 29th Annual AAS Guidance and Control Conference, Breckenridge, Colorado, Feb 4–8, 2006, in *Advances in the Astronautical Sciences*, Vol. 125, 2006. 2, 3, 4, 5, 6, 7, 8

[16] URL: http://www.acsinnovations.com/index_files/products.htm 2